

Amino-functionalized poly(L-lactide) lamellar single crystals as a valuable substrate for delivery of HPV16-E7 tumor antigen in vaccine development

Paola Di Bonito¹
 Linda Petrone¹
 Gabriele Casini²
 Iolanda Francolini²
 Maria Grazia Ammendolia³
 Luisa Accardi¹
 Antonella Piozzi²
 Lucio D'Ilario²
 Andrea Martinelli²

¹Department of Infectious, Parasitic and Immune-mediated Diseases, Italian National Institute of Health,
²Department of Chemistry, Sapienza University of Rome, Rome, Italy;
³Department of Technology and Health, Italian National Institute of Health, Rome, Italy

Correspondence: Paola Di Bonito
 Department of Infectious, Parasitic and Immune-mediated Diseases, Istituto Superiore di Sanità, Viale Regina Elena 288, 00161 Rome, Italy
 Tel +39 06 4990 2956
 Email paola.dibonito@iss.it

Andrea Martinelli
 Department of Chemistry, Sapienza University of Rome, Ple A Moro 5, 00185 Rome, Italy
 Tel +39 06 4991 3950
 Email andrea.martinelli@uniroma1.it

Background: Poly(L-lactide) (PLLA) is a biodegradable polymer currently used in many biomedical applications, including the production of resorbable surgical devices, porous scaffolds for tissue engineering, nanoparticles and microparticles for the controlled release of drugs or antigens. The surfaces of lamellar PLLA single crystals (PLLA_{sc}) were provided with amino groups by reaction with a multifunctional amine and used to adsorb an *Escherichia coli*-produced human papillomavirus (HPV)16-E7 protein to evaluate its possible use in antigen delivery for vaccine development.

Methods: PLLA single crystals were made to react with tetraethylenepentamine to obtain amino-functionalized PLLA single crystals (APLLA_{sc}). Pristine and amino-functionalized PLLA_{sc} showed a two-dimensional micro-sized and one-dimensional nano-sized lamellar morphology, with a lateral dimension of about 15–20 μm, a thickness of about 12 nm, and a surface specific area of about 130 m²/g. Both particles were characterized and loaded with HPV16-E7 before being administered to C57BL/6 mice for immunogenicity studies. The E7-specific humoral-mediated and cell-mediated immune response as well as tumor protective immunity were analyzed in mice challenged with TC-1 cancer cells.

Results: Pristine and amino-functionalized PLLA_{sc} adsorbed similar amounts of E7 protein, but in protein-release experiments E7-PLLA_{sc} released a higher amount of protein than E7-APLLA_{sc}. When the complexes were dried for observation by scanning electron microscopy, both samples showed a compact layer, but E7-APLLA_{sc} showed greater roughness than E7-PLLA_{sc}. Immunization experiments in mice showed that E7-APLLA_{sc} induced a stronger E7-specific immune response when compared with E7-PLLA_{sc}. Immunoglobulin G isotyping and interferon gamma analysis suggested a mixed Th1/Th2 immune response in both E7-PLLA_{sc}-immunized and E7-APLLA_{sc}-immunized mice. However, only the mice receiving E7-APLLA_{sc} were fully protected from TC-1 tumor growth after three doses of vaccine.

Conclusion: Our results show that APLLA single crystals improve the immunogenicity of HPV16-E7 and indicate that E7-APLLA_{sc} could be used for development of an HPV16 therapeutic vaccine against HPV16-related tumors.

Keywords: poly(L-lactide), lamellar crystals, human papillomavirus, HPV16-E7, therapeutic vaccine

Introduction

Vaccines based on recombinant and purified antigens require adjuvants and efficient delivery systems to induce an optimal immune response. Particulate antigens have recently been proposed for vaccine development. The intrinsic adjuvant properties of antigens in the form of microparticles and nanoparticles have been shown in several studies.^{1,2} One of the primary roles of particulate antigens in vaccination is their

effective uptake by antigen-presenting cells and subsequent delivery to lymphoid organs.^{1,2} Biodegradable polymers have also been widely investigated as vaccine adjuvants. They increase the bioavailability, half-life, and stability of the antigen while guaranteeing its safety for in vivo use and sustained and controlled delivery of the bound antigen.³

Polymeric systems based on particulate poly(L-lactide) (PLLA) or poly(lactide-co-glycolide) have been successfully employed to deliver antigens.⁴ These systems are able to activate humoral-mediated and cell-mediated immune responses by ensuring antigen presentation through the major histocompatibility complex I and II pathways. Several studies also show that the size and shape of particulate adjuvants affect the immune response.^{5–8} In fact, nanoparticles ranging from 10 to 500 nm can be taken up by macrophages and dendritic cells to promote antigen presentation. In particular, antigens conjugated to 50 nm nanoparticles are preferentially taken up by dendritic cells.⁹ These kinds of immunogens, which stimulate both humoral-mediated and CD8 T-cell-mediated immune responses, were able to reduce tumor burden in two different animal models.^{8,10}

Microparticulate polymers of 1–100 μm in size are useful for the controlled release of antigens and possibly reduce the number of vaccine doses required. They are currently used to develop monodose and needle-free mucosal vaccines. Microparticles deliver the antigens to microfold cells on mucosal surfaces after oral administration or to antigen-presenting cells after parenteral inoculation.²

Human papillomaviruses (HPVs) are epitheliotropic viruses responsible for the development of genital malignant diseases.¹¹ In particular, HPV16 is the main etiological agent of cervical cancer, being the cause of 61% of all cervical cancers in women worldwide.^{12,13} The virus is also involved in other anogenital and head and neck cancers.¹⁴ To prevent HPV infections in humans, two prophylactic HPV vaccines, based on recombinant virus-like particles, have been licensed and are currently used in humans. Both vaccines, Gardasil[®] and Cervarix[®], promote capsid-specific neutralizing antibodies against oncogenic HPV16 and HPV18, while Gardasil also protects against HPV11 and HPV6, which cause benign genital condylomas.¹⁵ Therapeutic vaccines that can treat established HPV infections by inducing a cell-mediated immune response have not yet been licensed for any genotype. Most of the therapeutic vaccines developed so far are based on the viral early oncoproteins E6 and E7.¹⁶ These proteins contain several reactive T-cell epitopes and play a role as tumor rejection antigens in humans. Vaccines based on E6 and E7 can be used for both preventing

and treating HPV-associated malignancies.^{17,18} Because of its poor immunogenic capability, due to its small size, E7 (11 kDa) was fused to different peptides and proteins, including HPV16-L1, HPV16-L2, and HPV16-E6, with the aim of combining prophylactic and therapeutic vaccines in a unique preparation. Although many developed therapeutic vaccines provided a good immune response in HPV16-related tumor regression in both animal and ex vivo human preclinical models, only a few of them have reached the clinical trial phase, and there are ongoing efficacy studies for their approval.^{17,18}

This investigation explores the use of pristine and surface amino-functionalized lamellar poly(L-lactide) single crystals (PLLA_{sc} and APLLA_{sc}, respectively), possessing a two-dimensional micro-sized, one-dimensional nano-sized lamellar morphology, as a delivery system for an *Escherichia coli*-expressed HPV16-E7.^{19,20} The chemical and physico-chemical properties of PLLA_{sc} and APLLA_{sc} were analyzed. The polymer lamellae were adsorbed with the E7 tumor antigen. E7-specific humoral-mediated, cell-mediated, and tumor-protective immune responses were evaluated in the HPV16 mouse tumor model, which uses the TC-1 cell line challenge in C57BL/6 mice.²¹ The results provide a novel delivery system for the development of an effective therapeutic vaccine against HPV16-associated tumors.

Materials and methods

Materials

The materials used in this study were all high purity reagents. PLLA (approximate molecular weight 152×10^3 g/mole), tetraethylenepentamine (TEPA), ninhydrin, dithiothreitol reducing agent, Tris, NaCl, NaH₂PO₄, Na₂HPO₄, sodium dodecyl sulfate (SDS), Tween 20, Triton X-100, Triton X-114, β -mercaptoethanol, bovine serum albumin, imidazole, glycerol, ethanol, isopropanol, acetic acid, geneticin (G418), sulfuric acid, and methanol were purchased from Fluka (Sigma-Aldrich Co., St Louis, MO, USA), Water Plus deionized water from Carlo Erba-Dasit (Cornaredo, Italy), and Ni-NTA resin from Qiagen NV (Venlo, the Netherlands). Ultrapure urea and glycine were from MP Biomedicals (Santa Ana, CA, USA). The acrylamide-bis-acrylamide (29:1) 30% Coomassie brilliant blue stain and colorimetric protein assay were from Bio-Rad Laboratories Inc. (Hercules, CA, USA). The primary antibodies and horseradish peroxidase secondary antibodies were from Pierce (Thermo Fisher Scientific, Waltham, MA, USA). The tetramethyl benzidine substrate was from Vector Laboratories Ltd (Peterborough, UK). The phosphate-buffered saline solution, fetal bovine serum, Roswell Park Memorial Institute

(RPMI) 1640 mammalian culture medium, and supplements were from Lonza Group Ltd (Basel, Switzerland). The bacterial culture medium and supplements were from Oxoid (Thermo Fisher Scientific). The mouse lymphocyte purification kit was from Life Technologies (Thermo Fisher Scientific, Waltham, MA, USA) and the interferon gamma (IFN- γ) ELISPOT kit was from Mabtech AB (Nacka Strand, Sweden). C57BL/6 mice were obtained from Charles River Laboratories (Wilmington, MA, USA). The aluminum specimen stubs used for scanning electron microscopy (SEM) were from Agar Scientific Elektron Technology Ltd (Stansted, UK) and the QCL-1000 Limulus amoebocyte lysate assay was from Lonza Group Ltd.

Preparation of PLLA_{sc} and surface aminolysis reaction

Lamellar PLLA_{sc} were prepared as previously reported.¹⁹ Briefly, PLLA was purified and crystallized from 0.25% (w/v) *p*-xylene solution at a T_c of 90°C according to the procedure described by Iwata and Doi.²² At the end of crystallization, the single crystals were collected by centrifugation and repeatedly washed first with cold *p*-xylene and then with ethanol, in which they were finally suspended.

To increase the adsorption of E7 oncogenic protein and to control its release, free amino groups were introduced onto the PLLA_{sc} surface by an aminolysis reaction with distilled TEPA. To avoid changes in the single crystal morphology, TEPA concentration, reaction time, and temperature were optimized. The PLLA_{sc} were suspended in 0.1 g/mL TEPA solution in isopropanol for 10 minutes at 55°C. The APLLA_{sc} were then repeatedly centrifuged and washed with isopropanol, in which they were finally suspended. The reaction product was characterized by Fourier transform infrared spectroscopy, differential scanning calorimetry, and water contact angle analysis. The concentration of free amino groups on the APLLA_{sc} surface was determined by ultraviolet-visible spectroscopy.

Attenuated total reflection Fourier transform infrared spectroscopy was performed on PLLA_{sc} and APLLA_{sc} samples using a Nicolet 6700 instrument (Thermo Fisher Scientific), equipped with a Golden Gate diamond single reflection device (Specac Ltd, Orpington, UK). The spectra were acquired by co-adding 200 interferograms in the range of 4,000–650 cm⁻¹ at a resolution of 2 cm⁻¹.

The effect of the aminolysis reaction on the thermal properties of PLLA_{sc} was studied by differential scanning calorimetry carried out using DSC822e apparatus (Mettler Toledo, Greifensee, Switzerland) in the temperature range of 30°C–200°C. The temperature runs were performed on

3–4 mg of sample under a nitrogen atmosphere at a heating rate of 10 K per minute.

The increase in surface hydrophilicity of PLLA due to the aminolysis reaction was verified by measuring the water wettability of pristine and amino-functionalized polymer films, as the single crystals are too small to be directly tested. The aminolysis reaction was carried out on the films under the same conditions used for PLLA_{sc}.

Dynamic advancing (θ_a) and receding (θ_r) contact angles were measured at room temperature using a DCA-312 dynamic contact angle analyzer. Deionized water ($\gamma_w = 72.8$ mN/m) was used as a wetting medium in an immersion and withdrawal cycle performed at a stage speed of 60 μ m per second.

The amount of TEPA bonded to single crystals was determined by ultraviolet-visible spectroscopy carried out using an HP 8452A diode array spectrophotometer (Hewlett Packard, Palo Alto, CA, USA) according to the procedure described by Cui et al using ninhydrin as an amine-specific dye.²³ The concentration, expressed as moles per mg of APLLA_{sc} sample, was determined by means of a calibration curve obtained using known concentrations of distilled TEPA.

Expression, purification, and analysis of E7 protein

Histidine-tagged E7 protein was expressed and purified as previously described.^{20,24} Briefly, *E. coli* inclusion bodies containing histidine-tagged E7 protein were lysed in a denaturing buffer containing 8 M urea, 10 mM NaH₂PO₄, 10 mM Tris-HCl (pH 8), 300 mM NaCl, 1 mM dithiothreitol, 1% Triton X-114, and 1% Triton X-100 (Buffer B mode). After sonication and centrifugation at 10,000 rpm in an SS34 rotor (Sorvall centrifuge), the supernatant was incubated with 50% slurry Ni-NTA resin at room temperature for 30 minutes. To reduce the endotoxin content, the E7-Ni-NTA agarose suspension was sequentially washed in Buffer B without detergents, and containing 10% glycerol (100 mL), 20% ethanol (100 mL), and 60% isopropanol (200 mL). The isopropanol washes were alternated with 10 mM Tris-HCl washes (200 mL). The last wash was performed using 500 mL of Buffer C (8 M urea, 10 mM NaH₂PO₄, 10 mM Tris-HCl, pH 6.3). The protein was eluted using 500 mM imidazole in Buffer B. After an analytical Coomassie-stained SDS polyacrylamide gel electrophoresis (PAGE), the fractions containing the E7 protein were collected and the protein was subjected to two-step dialysis at 4°C in native buffer, the first containing 1 mM dithiothreitol.²⁰ The protein was quantified by standard colorimetric methods (bicinchoninic acid assay).

Its purity and identity were monitored by 12.5% polyacrylamide gels in Tris-glycine buffer (SDS-PAGE) followed by Coomassie brilliant blue staining. The protein samples were denatured in SDS-loading buffer (25 mM Tris-HCl pH 6.8, 5% β -mercaptoethanol, 2% SDS, 50% glycerol). The protein identity was verified by Western blot using specific antibodies.²⁵ The endotoxin contamination was as low as 0.5 EU/mg protein, as monitored by Limulus amoebocyte lysate assay. Transmission electron microscopy showed the protein assembled in particles in the 45–200 nm size range, as previously described.²⁰

E7 adsorption on PLLA_{sc} and APLLA_{sc} and protein release experiments

Pristine PLLA_{sc} or APLLA_{sc} samples (20 mg) were incubated for 24 hours at room temperature with 1 mL of an E7 protein solution (1 mg/mL) in Tris-NaCl buffer (pH 8) under gentle stirring. The samples were successively centrifuged at low speed (300× g) and washed twice with 1 mL of Tris-NaCl buffer to remove unbound E7. The quantity of E7 adsorbed on the PLLA_{sc} and APLLA_{sc} samples was estimated by SDS-PAGE after Coomassie brilliant blue staining of the gel and using known amounts of bovine serum albumin protein as a standard, as described in Casini et al.²⁶ The E7-containing samples were designated E7-PLLA_{sc} and E7-APLLA_{sc}. These complexes were used to immunize mice, as described in the Immunization and tumor protection experiments section.

For protein-release experiments, E7-PLLA_{sc} and E7-APLLA_{sc} suspensions (1 mL) containing about 100 μ g of E7 were washed five times with a 1 mL aliquot of phosphate-buffered saline (pH 7.3) in Eppendorf tubes by gently inverting the tube three times. After each wash, the particle suspensions were centrifuged at low speed (300× g), the supernatant was removed, and the protein released was quantified by colorimetric (bicinchoninic acid) protein assay in 10 μ L of supernatant.

Scanning electron microscopy analysis

The morphology of PLLA_{sc}, APLLA_{sc}, E7-PLLA_{sc} and E7-APLLA_{sc} was observed by ultra-high resolution field emission gun scanning electron microscopy (FEG-SEM, FEI Company, Hillsboro, OR, USA). Secondary electron images were acquired with an acceleration voltage of 10 kV. Before analysis, the samples were gold-sputtered. For SEM observations of non-loaded single crystals, a drop of lamellae suspension in isopropanol was deposited on an aluminum stub and the liquid was removed through evaporation. For the E7-loaded samples, an aliquot of E7-PLLA_{sc} or E7-APLLA_{sc}

suspension in phosphate-buffered saline containing the same sample amount used for subcutaneous mouse inoculation was deposited on an aluminum stub, dried, and used to analyze the morphology of the aggregated sample.

Semiquantitative analysis of the surface of aggregated structures of E7-PLLA_{sc} or E7-APLLA_{sc} was carried out by counting surface projections (crests) from at least 50 random fields of view for both samples at a magnification of 1,200×.

Immunization and tumor protection experiments

Female C57BL/6 mice (aged 6–8 weeks) were purchased from Charles River Laboratories and maintained in the animal facility at the Italian National Institute of Health under pathogen-free conditions for one week before the experiments. Two groups of mice (n=15 per group) were inoculated subcutaneously in the bottom right flank with three doses of 10 μ g of E7 bound to either PLLA_{sc} or APLLA_{sc} at one-week intervals. Each dose contained about 33 mg of biodegradable polymer, corresponding to 10 μ g of bound E7. The same dose schedule was adopted for treating one group of mice (n=15 per group) subcutaneously with three doses of 10 μ g free E7.²⁰ A fourth mouse group was inoculated with saline solution and used as a control (naïve). Two other groups of mice were inoculated only with 33 mg of pristine PLLA and APLLA without protein.

Two weeks after the last immunization, five mice in each group were euthanized to analyze the immune response, and ten mice were inoculated subcutaneously with 1×10^5 TC-1 tumor cells per mouse. TC-1 cells are primary lung epithelial cells derived from C57BL/6 mice and transformed with the *HPV16 E6*, *E7* and *c-Ha-ras* genes.²¹ These cells are able to induce a palpable tumor when inoculated in the lower right flank of the mouse. TC-1 cells, cultured in RPMI 1640 supplemented with 10% fetal calf serum, 1% penicillin/streptomycin, 2 mM glutamine, 1 mM pyruvate, and 1% non-essential amino acids were selected in G418 0.4 mg/mL. Cells at 50% confluence were harvested, counted, and rinsed in Hank's medium at 1×10^6 cells/mL for injection into the mice. The challenge dose used was 1×10^5 cells/mouse (100 μ L). Tumor growth was monitored by visual inspection and palpation once a week for 2 months. After this time interval, the mice were euthanized. The immunization and tumor protection experiment was performed three times.

The experiments with animals have been made minimizing any possible suffering according to the Ethical Committee of the Istituto Superiore di Sanità, Rome, Italy (protocol

555/SA/2012) and according to Legislative Decree 116/92 which has implemented in Italy the European Directive 86/609/EEC on laboratory animal protection.

Antibody assay

The sera from each group of immunized mice were pooled and analyzed after the second and third dose of immunogens. To determine the anti-E7 specific immunoglobulin (Ig)G titer, the sera pools were serially diluted (two-fold and ten-fold) and assayed by enzyme-linked immunosorbent assay.²⁵ The endpoint dilution corresponded to an optical density absorbance <0.1 at 450 nm. Sera pools diluted 1:100 were used to analyze anti-E7 IgM, IgA and IgG isotypes (IgG1, IgG2b, IgG2c, and IgG3). Antigen-antibody complexes were detected using the following horseradish peroxidase secondary antibodies (Sigma-Aldrich): rabbit anti-mouse IgG (H + L), goat anti-mouse IgM (μ -chain specific), goat anti-mouse IgA (α -chain specific), and goat anti-mouse IgG1, IgG2b, IgG2c, and IgG3. Horseradish peroxidase activity was revealed using tetramethyl benzidine in the presence of H_2O_2 . After 30 minutes at room temperature, the enzymatic reaction was stopped by adding 1 M sulfuric acid (50 μ L per well). Washing steps were done using 400 μ L per well of phosphate-buffered saline containing 0.05% Tween-20 in an automatic washer.

IFN- γ ELISPOT assay

Splenocytes from mice of the same immunization group were pooled and enriched in CD4⁺ and CD8⁺ cells using the Dynal mouse T-cell negative isolation kit. Cells were cultured in RPMI 1640 supplemented with 10% fetal calf serum, 1% penicillin/streptomycin, 2 mM glutamine, 1 mM pyruvate, and 1% non-essential amino acids (complete RPMI). The splenocyte pools (2×10^5 cells per well) were

stimulated for 5 days with 5 μ g/mL of two E7-CTL peptides, DLYCYEQL (21–28 amino acids) and RAHYNIVTF (49–57 amino acids). The IFN- γ ELISPOT assay was performed using commercially available reagents. Splenocytes enriched with T-cells were seeded in triplicate (5×10^5 cells per well) in 100 μ L of complete medium with the E7 stimulator peptides. After 18 hours at 37°C in a humidified 5% CO₂ incubator, the plates were analyzed for the presence of IFN- γ according to the manufacturer's protocol. Splenocytes stimulated with an unrelated mixture of peptides or mitogens were used as the negative and positive control, respectively.²⁷

Statistical analysis

The statistical analysis was performed using the Student's *t*-test for unpaired data. Differences were considered to be statistically significant at $P < 0.05$.

Results

Synthesis and characterization of PLLA_{sc}

PLLA_{sc} grown from *p*-xylene solution at 90°C had a lozenge or trunked lozenge shape with a lateral dimension of about 20–30 μ m, as observed by SEM (Figure 1A). Since it was not possible to determine the lamellar thickness, a value of about 12 nm, reported in the literature for PLLA_{sc} obtained under the same experimental conditions used here, was considered.²⁸ Our lamellar systems were well separated with a smooth surface and did not show any sheaf-like aggregation. PLLA, like most semicrystalline polymers, can form single crystals with a well-defined architecture, characterized by an ordered inner layer sandwiched between two amorphous regions consisting of chain folding and cilia, ie, terminal segments. The good accessibility and reactivity of the outermost lamellar surface allows the introduction of suitable functional groups. In addition, the compact and continuous crystalline

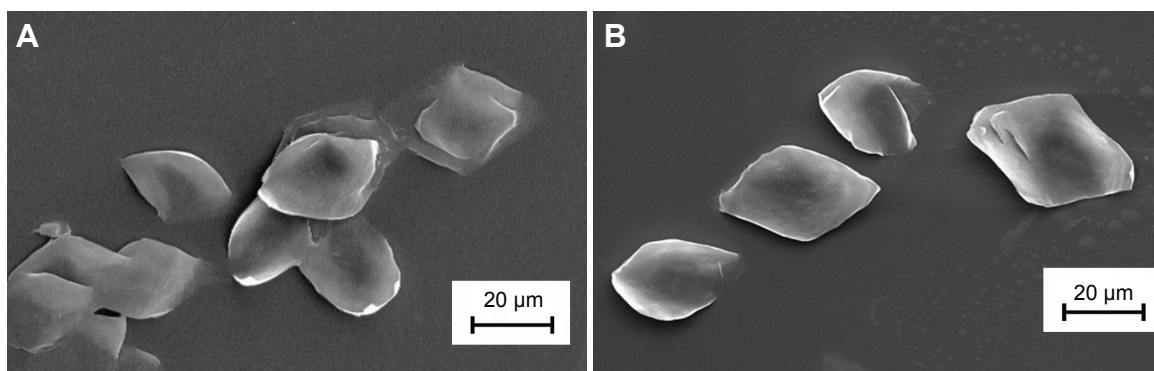


Figure 1 Scanning electron micrographs of PLLA_{sc} (A) and APLLA_{sc} (B).

Notes: A drop of PLLA_{sc} and APLLA_{sc} suspensions in isopropanol was deposited on the sample holder. The magnitude scale bars are indicated.

Abbreviations: PLLA_{sc}, poly(L-lactide) single crystals; APLLA_{sc}, amino-functionalized poly(L-lactide) single crystals.

core ensures the system's morphological and mechanical stability. These properties are of key importance in drug delivery applications where the precise control of chemical or biochemical parameters as well as specific physicochemical features (particle size, surface roughness, and composition) are needed.

In order to evaluate the effect of surface chemistry on E7 protein absorption and immunogenicity, the PLLA_{sc} surface was endowed with amino groups by an aminolysis reaction between PLLA_{sc} and a multifunctional amine, TEPA. This reaction can provide the lamella surface not just with amino groups but with hydroxyl functionalities as well, without producing any hydrolysis side reaction.²⁹

The aminolysis reaction conditions chosen in this study (0.1 g/mL TEPA solution in isopropanol, 10 minutes at 55°C), did not change the single crystal morphology or surface roughness, as shown by SEM images of well dispersed PLLA_{sc} and APLLA_{sc} lamellae, obtained from a diluted isopropanol suspension (Figure 1A and B). In contrast, more drastic reaction conditions (such as longer reaction time, and a higher temperature and amine concentration) brought about a reduction in the lamellar lateral dimension or weakening of the crystal structure with lamellar fragmentation in subsequent treatments (data not shown).

Because of the very high specific surface area of our system, the aminolysis reaction may be conveniently observed by attenuated total reflection Fourier transform infrared spectroscopy. PLLA_{sc} and APLLA_{sc} sample spectra are shown in Figure 2A.

The APLLA_{sc} spectrum, compared with that of pristine lamellae showed the presence of an additional absorption peak centered at about 1,620 cm⁻¹. This peak, due to amide C=O stretching and N-H bending, was found to be large because of the superimposition of various unresolved possible contributions, all resonating in the same spectral region.

In fact, according to steric hindrance considerations, the formation of a primary amide involving the TEPA terminal NH₂ could be favored, although the presence of a secondary amide cannot be excluded. Moreover, the hydrogen bond between the amide C=O group and TEPA protons could cause a red shift in the stretching absorption frequency.

The TEPA concentration on weighted amounts of APLLA_{sc} was determined by ultraviolet-visible spectroscopy at 515 nm employing a ninhydrin solution. A mean concentration of $(13 \pm 3) \times 10^{-6}$ mol of TEPA per gram of APLLA_{sc} was calculated.

In order to determine the reaction yield, the following issues were considered: in PLLA_{sc} the polymer chain axis is perpendicular to the lamella basal plane; the polymer crystallizes in the α form, consisting of two chains with 10₃ helical conformation packed into an orthorhombic cell with $a=1.07$ nm, $b=0.645$ nm, and $c=2.78$ nm; and one half of the aminolysed chains forms an amide bond with TEPA. Therefore, a maximum concentration of reaction sites for TEPA equal to 3×10^{-4} mol/g (equivalent to 2.3×10^{-6} mol/m²) can be inferred. This value allowed us to calculate a reaction yield of about 4.3%. In aminolysis reactions, reported in the literature and carried out on a PLLA membrane using hexamethylenediamine, the high hexamethylenediamine concentration of $1.6\text{--}2 \times 10^{-3}$ mol/m² was justified by polymer film roughness or porosity.³⁰ The aminolysis reaction deeply affected the thermal properties of PLLA_{sc} as shown in Figure 2B, where the differential scanning calorimetry heating profiles of pristine PLLA_{sc} and APLLA_{sc} are reported.

The pristine PLLA_{sc} thermogram showed an endothermic process at 168°C arising from the melting of original metastable crystals followed by a recrystallization process at 173°C that caused the formation of crystals with a thicker structure and melting at 183°C.³¹ As a result of the aminolysis reaction, the temperature of both the melting peaks decreased

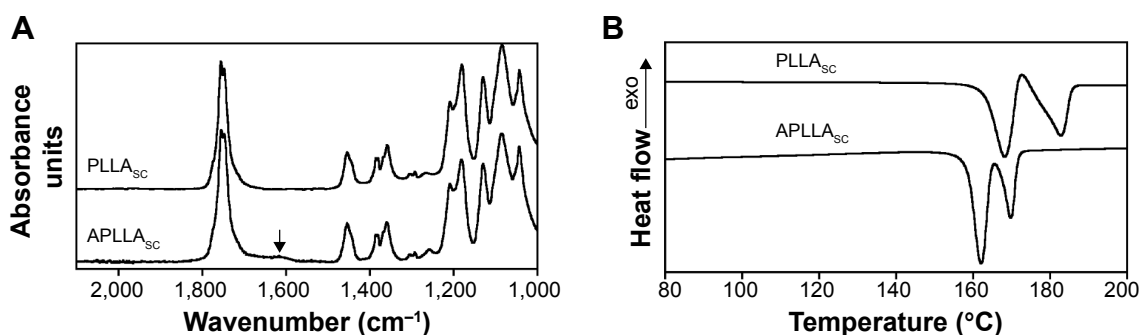


Figure 2 Attenuated total reflection Fourier transform infrared spectra of PLLA_{sc} and APLLA_{sc} (A). Differential scanning calorimetry thermograms of PLLA_{sc} and APLLA_{sc} recorded at 10°C per minute (B).

Note: The arrow indicates the amide C=O stretching and N-H bending large peak (A).

Abbreviations: PLLA_{sc}, poly(L-lactide) single crystals; APLLA_{sc}, amino-functionalized poly(L-lactide) single crystals.

and the small exothermic peak at about 173°C disappeared, since the shortest polymer chains involved in the reaction with TEPA cannot undergo the reorganization process. Similar thermal behavior has been already observed on hydrolyzed PLLA_{sc}.¹⁹ Moreover, since the overall enthalpy of fusion of the PLLA_{sc} and APLLA_{sc} samples ($\Delta H_m^{PLLA} = 72$ J/g, $\Delta H_m^{APLLA} = 70$ J/g, calculated by taking into account the integral of all the endothermic and exothermic processes) did not significantly change, it is possible to state that the inner crystalline cores of the single crystals were not involved in the aminolysis reaction.

Since the introduction of primary and secondary amino and hydroxyl groups on PLLA_{sc} by the TEPA aminolysis reaction can increase polymer surface hydrophilicity, the wettability of samples was evaluated by water contact angle measurements. PLLA films were used in these experiments because the single crystals are too small to be directly analyzed. Film aminolysis was carried out under the same reaction conditions used to prepare APLLA_{sc}.

The mean values of the dynamic advancing (θ_a) and receding (θ_r) contact angles and their hysteresis ($\Delta\theta = \theta_a - \theta_r$) for pristine PLLA and APLLA films are reported in Table 1. The data are representative of at least five independent experiments. Both θ_a and θ_r contact angles showed that the amino-functionalized sample was more hydrophilic than pristine PLLA. The low APLLA receding angle ($\theta_r = 5^\circ$) indicated nearly complete sample wettability. The high contact angle hysteresis found in the two samples can be ascribed to physicochemical surface heterogeneity. Such heterogeneity can be related to the presence of amorphous and crystalline areas as well as to the inhomogeneous distribution of the hydrophilic amino and hydroxyl groups in the functionalized sample.^{32,33}

HPV16-E7 protein adsorption and release

APLLA_{sc} or PLLA_{sc} were incubated in an HPV16-E7 protein solution to generate E7-APLLA_{sc} or E7-PLLA_{sc} complexes as described in the Materials and methods section. The amount, structural integrity, and stability of the E7 protein adsorbed on

pristine PLLA_{sc} and APLLA_{sc} were analyzed by SDS-PAGE (data not shown).²⁶ Despite the different chemical surface composition, the two E7-loaded samples bound similar quantities of protein. In particular, a value of 300 ± 30 ng of E7 per mg of APLLA_{sc} or PLLA_{sc} was determined as described in Casini et al.²⁶ Nevertheless, the protein released from the two substrates by controlled wash steps was different (Figure 3). In fact, a suitable quantity of either E7-APLLA_{sc} or E7-PLLA_{sc} complexes was repeatedly rinsed (five times) with 1 mL aliquots of phosphate-buffered saline. The released protein in the supernatants was determined after every rinsing step, as described in the Materials and methods section. The cumulative release fraction, expressed as $M(n)/M_0$, where M_0 is the amount of adsorbed protein at the beginning and $M(n)$ is the protein released at the n wash number, is reported in Figure 3. The results clearly show that the E7-PLLA_{sc} complex (solid line) released much more protein when compared with E7-APLLA_{sc} (dotted line) after each wash step. In particular, E7-PLLA_{sc} lost about 80% of the protein at the end of the washing step; in contrast, E7-APLLA_{sc} released only about 25% of protein during the same treatment.

As far as the morphology of the lamellae aggregates is concerned, it was observed that E7-APLLA_{sc} and E7-PLLA_{sc} showed different behavior on analysis of the SEM micrographs when a drop of the particulate suspension was dried on an aluminum stub (Figure 4). Both E7-PLLA_{sc} (Figure 4A) and E7-APLLA_{sc} (Figure 4B) showed a homogeneous layer characterized by a rough surface with lamellar structures projecting from the surface (crests). However, the E7-PLLA_{sc} surface was smoother and more compact than the rough and

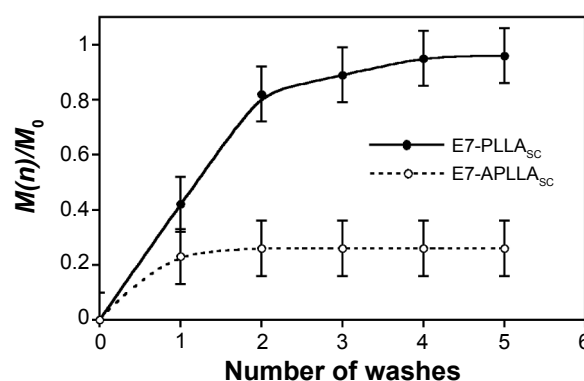


Figure 3 Protein release experiment.

Notes: E7-PLLA_{sc} and E7-APLLA_{sc} suspensions were centrifuged and rinsed in phosphate-buffered saline five times. The released E7 was quantified in the supernatant after each rinse step. The y axis reports the cumulative quantity of E7 released with respect to that initially adsorbed on the PLLA substrates. The x axis indicates each single wash step. The values are the mean of three determinations.

Abbreviations: PLLA, poly(L-lactide); E7-PLLA_{sc}, E7-containing poly(L-lactide) single crystals; E7-APLLA_{sc}, E7-containing amino-functionalized poly(L-lactide) single crystals.

Table 1 Advancing and receding contact angles of pristine and APLLA films in water measured using a stage speed of 60 μ m per second

| Sample | θ_a (°) | θ_r (°) | $\Delta\theta = \theta_a - \theta_r$ (°) |
|--------------------|----------------|----------------|--|
| Pristine PLLA film | 96.2 \pm 0.2 | 29 \pm 5 | 67 \pm 5 |
| APLLA film | 85 \pm 2 | 5 \pm 3 | 80 \pm 5 |

Note: The data are reported as the mean \pm standard deviation (n=5).

Abbreviations: PLLA, poly(L-lactide); APLLA, amino-functionalized poly(L-lactide).

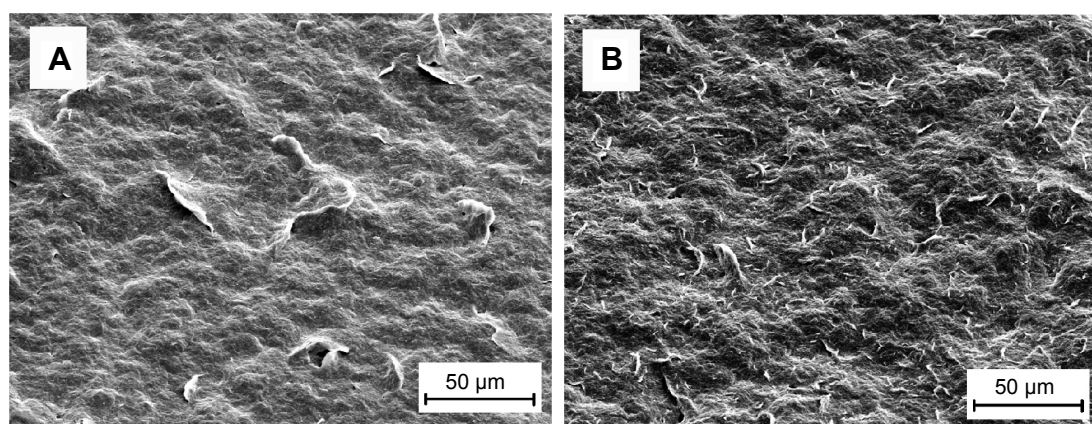


Figure 4 Scanning electron micrographs of E7-PLLA_{sc} (A) and E7-APLLA_{sc} (B) aggregates.

Notes: A drop of either E7-PLLA_{sc} or E7-APLLA_{sc} suspension, with the same concentration employed for subcutaneous mouse immunization, was deposited on the sample holder. The magnitude scale bars are indicated.

Abbreviations: E7-PLLA_{sc}, E7-containing poly(L-lactide) single crystals; E7-APLLA_{sc}, E7-containing amino-functionalized poly(L-lactide) single crystals.

nubby E7-APLLA_{sc} sample. Semiquantitative analysis of the crests on the surface, performed as described in the Materials and methods section, demonstrated that E7-APLLA_{sc} displayed 6–7-fold more crests than E7-PLLA_{sc} (Figure 4 and data not shown). The size of the crests ranged from about 5 to 15 µm for E7-APLLA_{sc} and from about 20 to 50 µm for E7-PLLA_{sc}. These findings suggest a different degree of aggregation of the two samples when subjected to the drying process. Probably, the formation of a continuous and compact layer in PLLA_{sc} was favored by interlamellar surface hydrophobic interactions. In contrast, electrostatic repulsion and surface hydrophilicity of APLLA_{sc} hampered tight lamella aggregation, promoting formation of a rough and porous layer with a greater available surface area.

Induction of the E7-specific immune response

Preliminary studies were performed to assess the toxicity, vaccine dose, and schedule vaccination for PLLA_{sc} and APLLA_{sc} in C57BL/6 mice. Acute toxicity tests performed in these mice showed that PLLA_{sc} and APLLA_{sc} were not toxic to animals at a dose up to 5 mg/g of mouse body weight when administered by the subcutaneous or intraperitoneal route. In these conditions, neither death nor changes in physiological behavior were observed in the treated animals. Moreover, we did not detect any anti-PLLA antibodies in mouse serum. In addition, neither an anti-E7-specific immune response nor tumor protection after HPV16-dependent tumor challenge (data not shown) were induced by the polymers. In a previous study, it was demonstrated that three 10 µg doses of E7 per mouse, composed of protein in particle forms of 45–200 nm (free E7), were necessary to induce humoral-mediated and

cell-mediated immune responses able to protect mice from TC-1 tumor challenge.²⁰ To investigate if the PLLA substrates had any adjuvant activity able to improve a specific immune response of free E7, groups of mice were inoculated three times with free E7 adsorbed on either PLLA_{sc} or APLLA_{sc}, as described in the Materials and methods section. Two weeks after the last immunization, the E7-specific antibody and cell-mediated immune responses were analyzed in a proportion of the animals in each immunization group. The remaining animals in each group were challenged subcutaneously with TC-1 tumor cells to evaluate the protective immune response against the engraftment of tumor cells and tumor growth. To quantify the humoral immune response and to compare the IgG antibody levels obtained in the animals, the sera from each group were pooled and the antibody titers were determined by endpoint dilution in an E7-based IgG enzyme-linked immunosorbent assay, after the second and third immunization with the E7 particle preparations (Table 2). The anti-E7 IgG antibody response increased after the second and third doses of E7-APLLA_{sc}, free E7, and E7-PLLA_{sc} whereas no anti-E7 antibody response was detected after

Table 2 Sera pool titration by endpoint dilution ELISA of antibodies against E7 after the second and third doses of vaccine

| Antigen | Dose 2 | Dose 3 |
|------------------------|----------|----------|
| E7-APLLA _{sc} | 1:16,000 | 1:32,000 |
| E7-PLLA _{sc} | 1:2,000 | 1:4,000 |
| E7 | 1:4,000 | 1:8,000 |
| APLLA _{sc} | 1:1 | 1:1 |
| PLLA _{sc} | 1:1 | 1:1 |

Note: The endpoint titer was an optical density of 0.1.

Abbreviations: PLLA_{sc}, poly(L-lactide) single crystals; APLLA_{sc}, amino-functionalized poly(L-lactide) single crystals.

immunization with APLLA_{sc} or PLLA_{sc} only (Table 2). At the end of the vaccination period, the serum pool from mice inoculated with E7-APLLA_{sc} had the highest anti-E7 IgG titer (1:32,000), whereas the serum pools of mice immunized with free E7 or E7-PLLA_{sc} showed antibody titers of 1:8,000 and 1:4,000, respectively. These results show that only the APLLA_{sc} was able to improve the humoral response elicited by E7. Conversely, the presence of pristine PLLA_{sc} seems to be detrimental for E7 immunogenicity.

The presence of IgM and IgA, driving IgG induction and mucosal immunity, respectively, was also analyzed. Significant IgM levels were detected only in serum pools from mice immunized with APLLA_{sc}-E7 or free E7. The IgM levels of these two immunization groups were compared by endpoint dilution E7-based enzyme-linked immunosorbent assay. Notably, the IgM titer in the serum pool from E7-APLLA_{sc}-treated mice (1:1,000) was higher than the IgM titer in the serum pool from free E7-treated mice (1:200). The IgA titers were undetectable in the serum pools from all the groups of mice (data not shown). The titers reported above are the mean values of three experiments with sera pools. Overall, the results show that the IgG class of immunoglobulins was the predominant component of the humoral immune response in the three groups of mice.

The effector functions of IgG depend on its subclasses, which are also indicative of a Th1 or Th2 polarization of the immune response. Therefore, to better evaluate the E7-specific humoral immune response, the anti-E7 specific IgG1, IgG2b, IgG2c (corresponding to IgG2a in the C57BL/6 mouse strain), and IgG3 antibody subclasses were determined in the serum pools. An enzyme-linked immunosorbent assay result, included in Figure 5, shows that IgG2b and IgG2c levels were induced in all mouse groups. The anti-E7 IgG1 levels detected were higher in the serum pools of mice immunized with either E7-APLLA_{sc} (Figure 5, black bar) or E7-PLLA_{sc} (Figure 5, gray bar) compared with the sera of mice immunized with free E7 (Figure 5, white bar). E7-specific IgG3 values were undetectable in the serum pools of all immunization groups. These results show that a mixed Th1/Th2 immune response was elicited in all groups of mice treated with E7-APLLA_{sc}, E7-PLLA_{sc}, or free E7. Overall, the animals immunized with E7-APLLA_{sc} showed the highest induction of E7-specific antibody responses among the groups of mice analyzed (IgG, Figure 5, black bar).

To analyze the induction of the cell-mediated immune response, T-enriched splenocytes from different immunization groups of mice were stimulated *in vitro* either with two recall E7-CTL peptides (pE7) or with an unrelated mixture of peptides

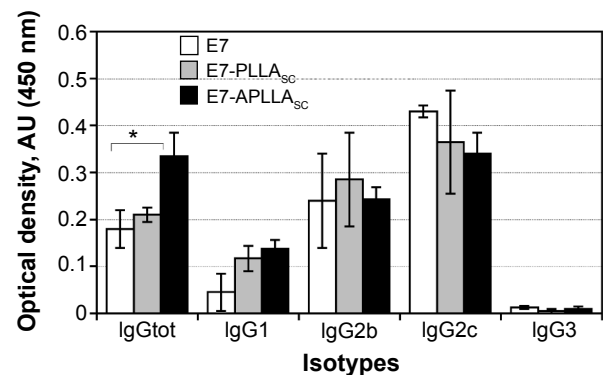


Figure 5 Determination of immunoglobulin isotypes by enzyme-linked immunosorbent assay.

Notes: The E7-specific IgG1, IgG2b, IgG2c and IgG3 immune reactivity is shown in OD₄₅₀ values on the y axis. The bars represent pools from sera of mice groups immunized with free E7 (E7, white bars), E7-PLLA_{sc} (gray bars), and E7-APLLA_{sc} (black bars). The four isotypes are indicated on the x axis along with the result of a total IgG enzyme-linked immunosorbent assay performed in parallel as control using the same serum pools. *Statistically significant result ($P < 0.05$).

Abbreviations: E7-PLLA_{sc}, E7-containing poly(L-lactide) single crystals; E7-APLLA_{sc}, E7-containing amino-functionalized poly(L-lactide) single crystals; Ig, immunoglobulin.

as a control, and then processed for an IFN- γ ELISPOT assay. The results of a representative experiment are shown in Figure 6. Significant amounts of IFN- γ -secreting cells were detected in T-enriched splenocytes from all three immunization groups, ie, E7-APLLA_{sc} ($P=0.009$), E7-PLLA_{sc} ($P=0.01$), and free E7 ($P=0.01$). A higher number of E7-specific IFN- γ -producing cells was detected in the E7-APLLA_{sc} group than in the group treated with free E7 (Figure 6). Instead, the lowest level of E7-specific IFN- γ -producing cells was detected in the E7-PLLA_{sc} group. The results show that all the immunogens used were able to induce a significant anti-E7-specific cell-mediated immune response, although to a different extent. Of note, the presence of pristine PLLA_{sc} was detrimental to

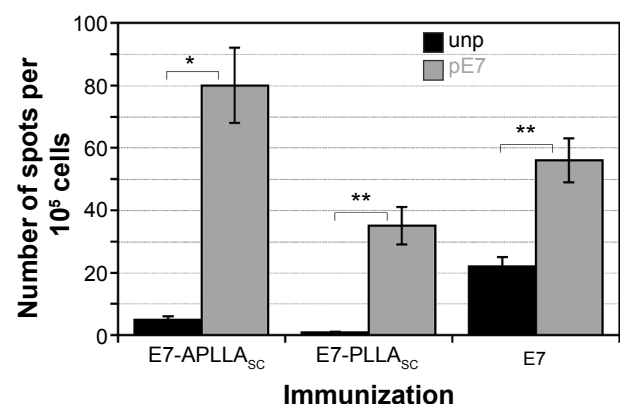


Figure 6 INF- γ -secreting cells from mice immunized with E7-APLLA_{sc}, E7-PLLA_{sc} and free E7 (E7).

Notes: The cells were stimulated with either an unrelated mixture of peptides (unp, black bars) or two CTLs E7 peptides (pE7, gray bars). * $P=0.009$; ** $P=0.01$.

Abbreviations: unp, unrelated mixture of peptides; pE7, E7 peptide; IFN- γ , interferon gamma; E7-PLLA_{sc}, E7-containing poly(L-lactide) single crystals; E7-APLLA_{sc}, E7-containing amino-functionalized poly(L-lactide) single crystals.

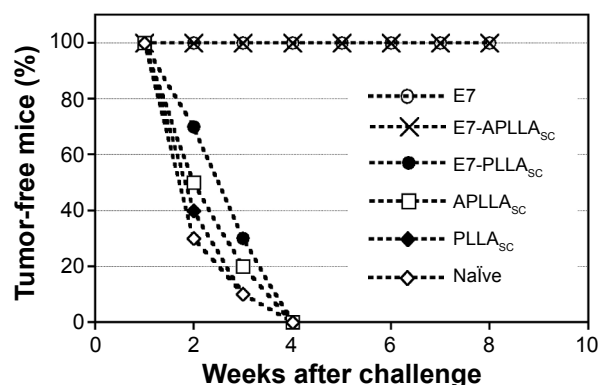


Figure 7 Tumor protection experiment.

Notes: Mice naïve or vaccinated with three doses of free E7 (E7), E7-APLLA_{sc}, E7-PLLA_{sc}, APLLA_{sc} and PLLA_{sc} were challenged with 1×10^5 TC-1 tumor cells and tumor growth was monitored weekly. The x axis indicates weeks of monitoring after tumor challenge and the y axis indicates the percentages of animals without tumor.

Abbreviations: E7-PLLA_{sc}, E7-containing poly(L-lactide) single crystals; E7-APLLA_{sc}, E7-containing amino-functionalized poly(L-lactide) single crystals.

induction of E7-specific T-cell immune responses, similar to what is observed for the antibody response.

To evaluate the efficacy of this anti-E7-specific cell-mediated immune response in the protection of mice from HPV16-dependent tumor development, the mice were challenged with TC-1 tumor cells after the immunization protocol and tumor growth was monitored for 2 months after the challenge.²¹ The results of a representative experiment are shown in Figure 7. Only mice vaccinated with either E7-APLLA_{sc} or free E7 were fully protected from tumor growth throughout the observation period. In contrast, mice immunized with E7-PLLA_{sc}, as well as mice in the control groups immunized with the APLLA_{sc} or PLLA_{sc} particles only and naïve mice developed a palpable tumor (Figure 7) within 4 weeks of tumor growth monitoring.

Discussion

During the last decade, several polymer particulate carriers have been shown to have intrinsic adjuvant activity when added to vaccine formulations to improve the immune response.^{1–3} However, safety concerns restrict the number of suitable materials, and further research is required to demonstrate the absence of risks as well as the real benefits to human health.^{34,35} Biodegradable and biocompatible polyesters are an interesting class of substrates because many of them, including poly(L-lactide) and its copolymers, have regulatory approval for some applications in humans, being degraded in the body into endogenous products by non-enzymatic hydrolysis.^{36,37}

In this paper, we compared the properties of pristine PLLA_{sc} and APLLA_{sc} and showed that both adsorbed large amounts of HPV16-E7 protein. However, when used in

immunogenicity studies in mice, only APLLA_{sc} demonstrated useful features for use in therapeutic vaccine development.

The lamellar PLLA_{sc} surface was amino-functionalized to obtain a cationic carrier for HPV16-E7 and possibly to increase adsorption by negative E7 charges. However, the amount of E7 adsorbed on pristine PLLA_{sc} and APLLA_{sc} was similar in our conditions. In contrast, the release of E7 protein in phosphate-buffered saline from APLLA_{sc} and PLLA_{sc} was different. The results showed that E7-APLLA_{sc} released much less E7 protein than E7-PLLA_{sc} in the same experimental conditions.

E7 adsorption on PLLA_{sc} and APLLA_{sc} substrates could likely be driven by hydrophobic or hydrogen bond/electrostatic interactions, respectively, which could affect the conformation of the adsorbed E7. Even though the E7 protein used in our experiments was in particulate form,²⁰ SEM analyses did not reveal any E7 particles on either APLLA_{sc} or PLLA_{sc} (data not shown), suggesting that a conformational change or some degree of aggregation occurred after protein–substrate interaction and protein adsorption. The poor elution of E7 from the APLLA_{sc} substrate in vitro could indeed suggest slow release of the antigen when the complex is subcutaneously inoculated as a vaccine in vivo.

The significant quantity of about 300 ng of E7 per mg of lamellae was related to the highly specific surface area of PLLA_{sc} or APLLA_{sc}, and corresponds to about 130 m²/g. Such a value was evaluated by geometrical calculations assuming a lamella thickness of 12 nm and a PLLA crystalline density equal to 1.285 g/cm³.^{22,31}

E7-APLLA_{sc} and E7-PLLA_{sc} aggregation was different when the samples were dried for SEM analyses. E7-PLLA_{sc} formed a compact layer of lamellar (piled-up) aggregates, probably due to hydrophobic interlamellae interactions. In contrast, the hydrophilic charged surface of APLLA_{sc} seemed to favor the formation of a rough and nubby layer. The different morphology of the dried E7-PLLA_{sc} and E7-APLLA_{sc} samples could reflect the real aggregation state of the antigen-polymer complexes when they are injected subcutaneously into animals. The greater roughness of E7-APLLA_{sc}, compared with E7-PLLA_{sc}, resulted in a greater surface area with E7 available to the antigen-presenting cells to establish immunity-inducing interactions.

The different behavior of E7-APLLA_{sc} and E7-PLLA_{sc} complexes observed in vitro could explain the better performance of the amino-functionalized substrate in the in vivo E7 immunogenicity study. In fact, lower antigen release and higher E7 surface availability could be responsible for the higher immunogenicity elicited by E7-APLLA_{sc} when

compared with PLLA_{sc} in C57BL/6 mice. It has already been shown that the low release of antigens achieved by microparticles is important for induction of strong and long-lasting immunity.³⁷ On the other hand, to maintain high levels of circulating antibodies, a small amount of antigen is sufficient once the primary immune response has been elicited.³⁷

Despite our interesting results, we cannot exclude the existence of other methodologies to adsorb HPV E7 protein on PLLA_{sc} surface preserving the E7 immunogenicity.

The analysis of the antibody response of mice immunized with E7 adsorbed on either pristine PLLA_{sc} or APLLA_{sc} showed that the strongest antibody response was obtained by immunization with E7-APLLA_{sc}, producing both IgGs and IgMs. The IgG antibodies were the predominant component of this humoral immune response. However, the induction of specific IgMs could play an important role by forming immune complexes with the antigen and acting like a self-adjuvant.³⁸

In our experiments, E7-specific IgG isotyping showed a pattern indicative of a mixed Th1/Th2 immune response. A significant cell-mediated immune response was also detected by IFN- γ ELISPOT assay in all mice groups analyzed. Of note, a higher percentage of IFN- γ -producing cells was detected in mice immunized with E7-APLLA_{sc} in comparison with those immunized with E7-PLLA_{sc}. The difference in T-cell immune response induction was certainly the cause of the different immune response to tumor challenge observed in the immunized mice. In fact, only the mice that received E7-APLLA_{sc} were fully protected from the tumor challenge, whereas those that received E7-PLLA_{sc} developed a tumor. It is worthy of note that pristine PLLA_{sc} reduces the immunogenicity of E7, thus it could represent a suitable substrate for the delivery of drugs where any possible substrate adjuvant activity should be avoided.

Conclusion

In this study, for the first time, HPV16-E7 was non-covalently loaded onto PLLA_{sc} to develop a vaccine against HPV16-related tumors. The results showed that only aminolysed PLLA induced an effective antibody and cell-mediated immune response, capable of protecting mice from challenge with tumor cells. These findings indicate that E7-APLLA_{sc} has the potential for use in the development of an HPV16 therapeutic vaccine.

Acknowledgments

We are grateful to Armando Cesolini and Andrea Giovannelli for their work with the animals. The research was supported by the Italian Ministry of Health, AIDS Project 2010, and by

Sapienza University of Rome funds. The present address for LP is INMI Lazzaro Spallanzani, Rome, Italy.

Disclosure

The authors report no conflicts of interest in this work.

References

1. Brito LA, O'Hagan DT. Designing and building the next generation of improved vaccine adjuvants. *J Control Release*. 2014;563–579.
2. Bolhassani A, Javanad S, Saleh T, Hashemi M, Aghasadeghi MR, Sadat SM. Polymeric nanoparticles: potent vectors for vaccine delivery targeting cancer and infectious diseases. *Hum Vaccin Immunother*. 2014;10:321–332.
3. Ahmed KK, Geary SM, Salem AK. Applying biodegradable particles to enhance cancer vaccine efficacy. *Immunol Res*. 2014;59:220–228.
4. Singh M, Kazzaz J, Ugozzoli M, Malyala P, Chesko J, O'Hagan DT. Polylactide-co-glycolide microparticles with surface adsorbed antigens as vaccine delivery systems. *Curr Drug Deliv*. 2006;3:115–120.
5. Oyewumi MO, Kumar A, Cui Z. Nano-microparticles as immune adjuvants: correlating particle sizes and the resultant immune responses. *Expert Rev Vaccines*. 2010;9:1095–1107.
6. Foge C, Brodin B, Frokjaer S, Sundblad A. Particle size and surface charge affect particle uptake by human dendritic cells in an in vitro model. *Int J Pharm*. 2005;298:315–322.
7. Agarwal R, Roy K. Intracellular delivery of polymeric nanocarriers: a matter of size, shape, charge, elasticity and surface composition. *Ther Deliv*. 2013;4:705–723.
8. Fifis T, Gamvrellis A, Crimeen-Irwin B, et al. Size-dependent immunogenicity: therapeutic and protective properties of nano-vaccines against tumors. *J Immunol*. 2004;173:3148–3154.
9. Hamdy S, Haddadi A, Hung RW, Lavasanifar A. Targeting dendritic cells with nano-particulate PLGA cancer vaccine formulations. *Adv Drug Deliv Rev*. 2011;63:943–955.
10. Jabbal-Gill I, Lin W, Jenkins P, et al. Potential of polymeric lamellar substrate particles (PLSP) as adjuvants for vaccines. *Vaccine*. 1999;18:238–250.
11. Zur Hausen H. Papillomavirus infections: a major cause of human cancer. In: Zur Hausen H, editor. *Infections Causing Human Cancer*. Weinheim, Germany: Wiley-VCH Verlag GmbH & Co KGaA; 2006:145–243.
12. Forman D, de Martel C, Lacey CJ, et al. Global burden of human papillomavirus and related diseases. *Vaccine*. 2012;30 Suppl 5:F12–F23.
13. De Sanjose S, Quint WG, Alemany L, et al. Human papillomavirus genotype attribution in invasive cervical cancer: a retrospective cross-sectional worldwide study. Retrospective international survey and HPV time trends study group. *Lancet Oncol*. 2010;11:1048–1056.
14. Syrjänen S. The role of human papillomavirus infection in head and neck cancers. *Ann Oncol*. 2010;21 Suppl 7:vii243–vii245.
15. Mariani L, Venuti A. HPV vaccine: an overview of immune response, clinical protection, and new approaches for the future. *J Transl Med*. 2010;8:105.
16. Moody CA, Laimins LA. Human papillomavirus oncoproteins: pathways to transformation. *Nat Rev Cancer*. 2010;10:550–560.
17. Su JH, Wu A, Scotney E, et al. Immunotherapy for cervical cancer: research status and clinical potential. *BioDrugs*. 2010;24:109–129.
18. van der Burg SH, Melief CJ. Therapeutic vaccination against human papilloma virus induced malignancies. *Curr Opin Immunol*. 2011;23:252–257.
19. D'Ilario L, Francolini I, Martinelli A, Piozzi A. Dipyrromethole-loaded poly(L-lactide) single crystals as drug delivery systems. *Macromol Rapid Commun*. 2007;28:1900–1904.
20. Petrone L, Ammendolia MG, Cesolini A, et al. Recombinant HPV16 E7 assembled into particles induces an immune response and specific tumor protection administered without adjuvant in an animal model. *J Transl Med*. 2011;9:69–77.

21. Lin KY, Guarnieri FG, Staveley-O'Carroll KF, et al. Treatment of established tumors with a novel vaccine that enhances major histocompatibility class II presentation of tumor antigen. *Cancer Res.* 1996; 56:21–26.
22. Iwata T, Doi Y. Morphology and enzymatic degradation of poly(L-lactic acid) single crystals. *Macromolecules.* 1998;31:2461–2467.
23. Cui W, Li X, Xie C, Zhuang H, Zhou S, Weng J. Hydroxyapatite nucleation and growth mechanism on electrospun fibers functionalized with different chemical groups and their combinations. *Biomaterials.* 2010;31:4620–4629.
24. Di Bonito P, Grasso F, Mangino G, et al. Immunomodulatory activity of a plant extract containing human papillomavirus 16-E7 protein in human monocyte-derived dendritic cells. *Int J Immunopathol Pharmacol.* 2009;22:967–978.
25. Di Bonito P, Grasso F, Mochi S, et al. Serum antibody response to human papillomavirus (HPV) infections detected by a novel ELISA technique based on denatured recombinant HPV16 L1, L2, E4, E6 and E7 proteins. *Infect Agent Cancer.* 2006;1:6.
26. Casini G, Petrone L, Bakry A, et al. Functionalized poly(L-lactide) single crystals coated with antigens in development of vaccines. 2010 CRS Annual Meeting. *J Control Release.* 2010;148:e106.
27. Di Bonito P, Grasso F, Mochi S, et al. Anti-tumor CD8⁺ T cell immunity elicited by HIV-1-based virus-like particles incorporating HPV-16 E7 protein. *Virology.* 2009;395:45–55.
28. Fujita M, Doi Y. Annealing and melting behavior of poly(L-lactic acid) single crystals as revealed by in situ atomic force microscopy. *Biomacromolecules.* 2003;4:1301–1307.
29. Croll TI, O'Connor AJ, Stevens GW, Cooper-White JJ. Controllable surface modification of poly(lactic-co-glycolic acid) (PLGA) by hydrolysis or aminolysis I: physical, chemical, and theoretical aspects. *Biomacromolecules.* 2004;5:463–473.
30. Zhu Y, Gao C, Liu X, Shen J. Immobilization of biomacromolecules onto aminolyzed poly(L-lactic acid) toward acceleration of endothelium regeneration. *Tissue Eng.* 2004;10:53–61.
31. Fischer EW, Sterzel HJ, Wegner GK. Investigation of the structure of solution grown crystals of lactide copolymers by means of chemical reaction. *Kolloid ZZ Polym.* 1973;251:980–990.
32. Park A, Cima LG. In vitro cell response to differences in poly-L-lactide crystallinity. *J Biomed Mater Res.* 1996;31:117–130.
33. Bakry A, Martinelli M, Bizzarri A, et al. A new approach for the preparation of hydrophilic poly(L-lactide) porous scaffold for tissue engineering by using lamellar single crystals. *Polym Int.* 2012;61:1177–1185.
34. Elsaesser A, Howard CV. Toxicology of nanoparticles. *Adv Drug Deliv Rev.* 2012;64:129–137.
35. Cattaneo AG, Gornati R, Sabbioni E, et al. Nanotechnology and human health: risks and benefits. *J Appl Toxicol.* 2010;30:730–744.
36. Palm MD, Goldman MP. Patient satisfaction and duration of effect with PLLA: a review of the literature. *J Drugs Dermatol.* 2009;8 Suppl 10: S15–S20.
37. Coombes AG, Lavelle EC, Davis SS. Biodegradable lamellar particles of poly(lactide) induce sustained immune responses to a single dose of adsorbed protein. *Vaccine.* 1999;17:2410–2422.
38. Pepponi I, Stylianou E, van Dolleweerd C, et al. Immune-complex mimics as a molecular platform for adjuvant-free vaccine delivery. *PLoS One.* 2013;8:e60855.

International Journal of Nanomedicine

Publish your work in this journal

The International Journal of Nanomedicine is an international, peer-reviewed journal focusing on the application of nanotechnology in diagnostics, therapeutics, and drug delivery systems throughout the biomedical field. This journal is indexed on PubMed Central, MedLine, CAS, SciSearch®, Current Contents®/Clinical Medicine,

Submit your manuscript here: <http://www.dovepress.com/international-journal-of-nanomedicine-journal>

Dovepress

Journal Citation Reports/Science Edition, EMBASE, Scopus and the Elsevier Bibliographic databases. The manuscript management system is completely online and includes a very quick and fair peer-review system, which is all easy to use. Visit <http://www.dovepress.com/testimonials.php> to read real quotes from published authors.